Proc. Nat. Acad. Sci. USA
Vol. 72, No. 5, pp. 1649–1653, May 1975

Conjugated Polyene Fatty Acids As Membrane Probes: Preliminary Characterization

(fluorescence/lipid–protein interactions/lipid phase transitions/ induced circular dichroism/energy transfer)

LARRY A. SKLAR, BRUCE S. HUDSON, AND ROBERT D. SIMONI

Departments of Chemistry and Biological Sciences, Stanford University, Stanford, Calif. 94305

Communicated by Harden M. McConnell, January 24, 1975

ABSTRACT **The use of fluorescent conjugated polyenoic fatty acids as probes of membrane structure is introduced. α- and β-parinaric acid (*cis, trans, trans, cis*-, and *all trans*-9,11,13,15-octadecatetraenoic acid) and synthetic lecithins containing an α-parinaric acid chain in position 2 are prepared and their absorption and fluorescence properties are determined.**

Phase transitions are detected as fluorescence changes at characteristic temperatures when either the free fatty acid probes or the labeled phospholipid probe are included in sonicated aqueous dispersions of L-α-dimyristoyl lecithin, L-α-dipalmitoyl lecithin, or L-α-distearoyl lecithin. The phase transitions are detected at about 23°C (dimyristoyl), 44°C (dipalmitoyl), and 53°C (distearoyl lecithin).

Binding of α-parinaric acid to bovine serum albumin is measured by shifts in the absorption spectrum and enhanced quantum yield of the fatty acid upon binding and by energy transfer between 2 tryptophyl residues in bovine serum albumin and α-parinaric acid. Approximately six binding sites are detected.

Other applications of these probe molecules, including phase transitions of phospholipid/cholesterol dispersions, induced circular dichroism of parinaric acid bound to albumin, and biosynthetic incorporation of parinaric acid into biological membranes, are discussed.

Fluorescence spectroscopy of molecular probes has provided much insight into the complexities of biological membranes (1–3). This report describes our initial efforts toward establishing the use of a unique class of fluorescent probes: polyunsaturated fatty acids in which the double bonds are conjugated. These molecules as a class are referred to as linear polyenes and are available with a variety of chain lengths and polyene positional and geometrical isomers. The structure and conformation of these molecules closely resembles that of normally occurring membrane fatty acids (Fig. 1). Environmental perturbations are expected to be minimal and the location and orientation of the chromophore relative to the surroundings is predictable. Recent studies of the electronic structure of linear polyenes (4) can be used to advantage in the application of their optical properties to membrane studies.

This paper reports the use of the two isomers of parinaric acid (9,11,13,15-octadecatetraenoic acid), namely the α isomer (*cis-trans-trans-cis*, I) and the β isomer (*all trans*, II) as well as lecithin derivatives of α-parinaric acid (III) in model system studies.

Abbreviations: Pal_2Lec, L-α-dipalmitoyl lecithin; Myr_2Lec, L-α-dimyristoyl lecithin; Ste_2Lec, distearoyl lecithin; CD, circular dichroism.

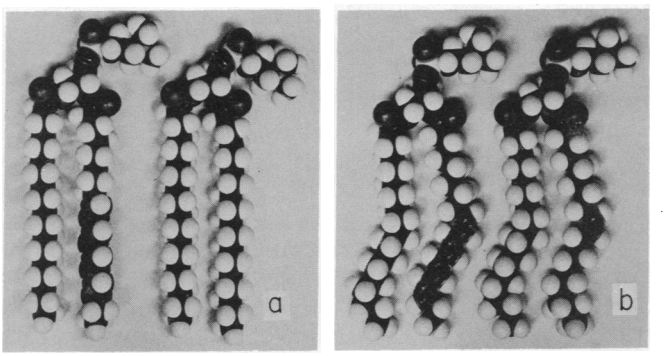

FIG. 1. CPK models of lecithins and parinaric-acid-labeled lecithins. Parinaric acid is attached to the 2 (or β) position (probe III, $n = 16$). (a) 1-Stearoyl, 2-β-parinaroyl lecithin, in which the polyene chain is *all-trans*, compared to the extended form of distearoyl lecithin. (b) 1-Stearoyl, 2-α(*cis-trans-trans-cis*)-parinaroyl lecithin compared to 1-stearoyl, 2-oleyl lecithin in which the oleyl chain is shown in a *gauche* conformation at C 15 and the stearoyl chains are in the *gauche* conformation at C9 and C15 for both models. The polyene-labeled lecithin is on the left in each case. The overall length of a polyene chain is nearly identical to that of an extended saturated chain when allowance is made for differences in both the bond lengths and bond angles.

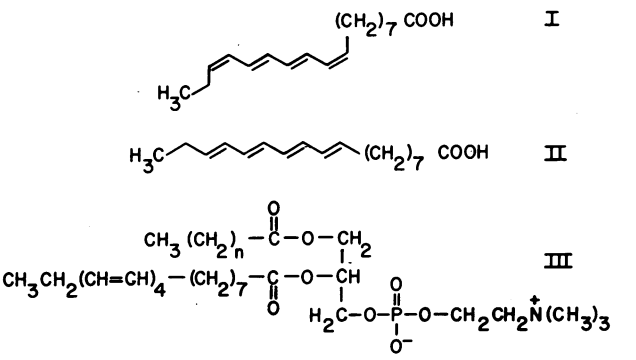

MATERIALS AND METHODS

Preparation of Fatty Acids. Fruits of the plant *Parinarium glaberrimum* [equivalent to *Parinarium laurimum* (5)] were obtained through the kind assistance of Mr. Koroiveibau of the Department of Agriculture, Fiji. α-Parinaric acid was isolated and purified essentially according to the procedure of Riley (6). Repeated recrystallization from petroleum ether (boiling range 38–58°C) yields white crystalline plates with

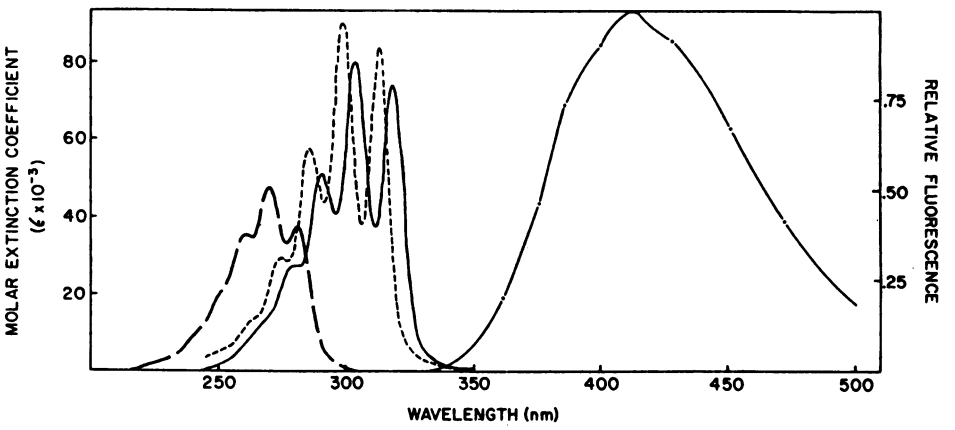

FIG. 2. Linear polyene spectra. The absorption spectra are shown for α-eleostearic acid (— —), α-parinaric acid (——), and β-parinaric acid (– – –). The fluorescence emission of α-parinaric acid (·—·), is shown as relative fluorescence, arbitrary units, scaled to 1.0 at the maximum at 410 nm (uncorrected spectrum). Excitation at 320 with slit width 3 nm and emission slit width 8 nm were used. Measurements were made in methanol at 25°C.

melting point 85–86°C, which contain less than 1% α-eleostearic acid as determined by gas–liquid chromatography (see below). The β isomer of parinaric acid was prepared by sunlight isomerization catalyzed by iodine (7, 8). Repeated recrystallization from hexane yields small white crystals with melting point 95–96°C and of purity greater than 99%. The purity of fatty acids was established by gas–liquid chromatography of the methyl esters prepared with Methyl-8 from Pierce Chemical Co. Analytical separations were performed on an F&M model 7000 gas chromatograph equipped with a flame detector using either a 6 ft × 1/8 inch column containing 20% diethylene glycol succinate (DEGS) on 80/100 Chromosorb W (8) or a 3 ft × 1/8 inch column containing 10% SP-2340 on 100/120 Supelcoport.

Preparation of Phospholipid Derivatives. Synthetic lecithins were prepared by a modification of the procedure of Cubero Robles and Van Den Berg (9). L-α-Distearoyl lecithin (Ste_2-Lec), L-α-dipalmitoyl lecithin (Pal_2Lec) and L-α-dimyristoyl lecithin (Myr_2Lec) were obtained from Calbiochem and used without further purification. Stearic acid (99+%, Chemical Sample Co.), palmitic acid (99%, Sigma), and myristic acid (99%, Aldrich) were used in the preparation of the sodium salts, and mixed anhydrides containing 1–10% α-parinaric acid. The lysolecithins were prepared in standard fashion and acylated in the presence of the salt and the mixed anhydride. The temperature for the reaction was kept in the 60–70°C range, and reaction times did not exceed 8 hr. The lecithins obtained had a degree of substitution in position 2 similar to the composition of the mixed anhydride used in the acylation. Silica gel column chromatography was used to purify the lecithins, and purity was checked by thin-layer chromatography.

Lipid Dispersions. Chloroform solutions containing 0.5 mg of the appropriate lipid plus 5 μg or less of the parinaroyl lecithin (III) were dried under vacuum in a small roundbottom flask. Dispersion in 5 ml of 0.01 M phosphate buffer, pH 7.5, was accomplished by brief sonication (60 sec, 50 W) under nitrogen with a Branson sonifier. Free polyene fatty acids were added after sonication in volumes of 1 μl of methanol per ml of buffer.

All of the above manipulations were performed under red light and under nitrogen. Fatty acids and the lecithin derivatives were stored in darkness at −20°C. Details of these preparative procedures will be discussed elsewhere.

Spectroscopy. Absorption spectra were recorded on a Cary 14 scanning spectrophotometer. Circular dichroism (CD) spectra were recorded on a Jasco J-40. Fluorescence spectra were recorded on an Hitachi-Perkin-Elmer model MPF-2A fluorimeter. Sample temperature was controlled by a circulating water bath connected to a jacketed cuvette and monitored inside the cuvette with a thermocouple thermometer. Samples were deoxygenated with nitrogen and allowed to equilibrate above their transition temperatures for at least 1/2 hr. Temperature was varied at 2°C/min. Absolute quantum yields were determined using 1,4-bis[2(4-methyl-5-phenyloxazolyl)]-benzene (dimethyl POPOP) in cyclohexane as a standard of quantum yield 0.93 (10).

RESULTS AND DISCUSSION

Spectral characteristics

Fig. 2 shows the absorption spectra of three polyene fatty acids in methanol and the fluorescence emission of α-parinaric acid at 25°C. α-Eleostearic acid (9,11,13-*cis,trans,trans*-octadecatrienoic acid) has its absorption maximum (270 nm) and weak fluorescence emission maximum (near 345 nm, not shown) in the same spectral regions as the absorption and fluorescence of tryptophan. α-Parinaric acid, with four double bonds, has absorption maxima at 303 nm ($\epsilon = 80 \times 10^3$), and 318 nm ($\epsilon = 74 \times 10^3$) and a broad emission spectrum with a maximum near 410 nm. The fluorescence quantum yield, Q, is 0.015 ± 0.003 in methanol. Since emission and the strong absorption involve different excited electronic states (4), the spectra are not mirror images and are widely separated so that self-absorption corrections are not required. The absorption strongly overlaps tryptophan emission, and the radius for 50% energy transfer is calculated to be 30 Å.* The absorption of the *trans* isomer, β-parinaric acid (maximum 299 nm, $\epsilon = 91 \times 10^3$), is also shown. The spectral differences between the two isomers are consistent with similar differences shown by other polyenes (12).

* Energy transfer calculation assumed $K^2 = 1$, $n = 1.4$, $Q = 0.4$, and from measurements $J \sim 10^{-14}$ cm^3 M^{-1}. For method, see ref. 11.

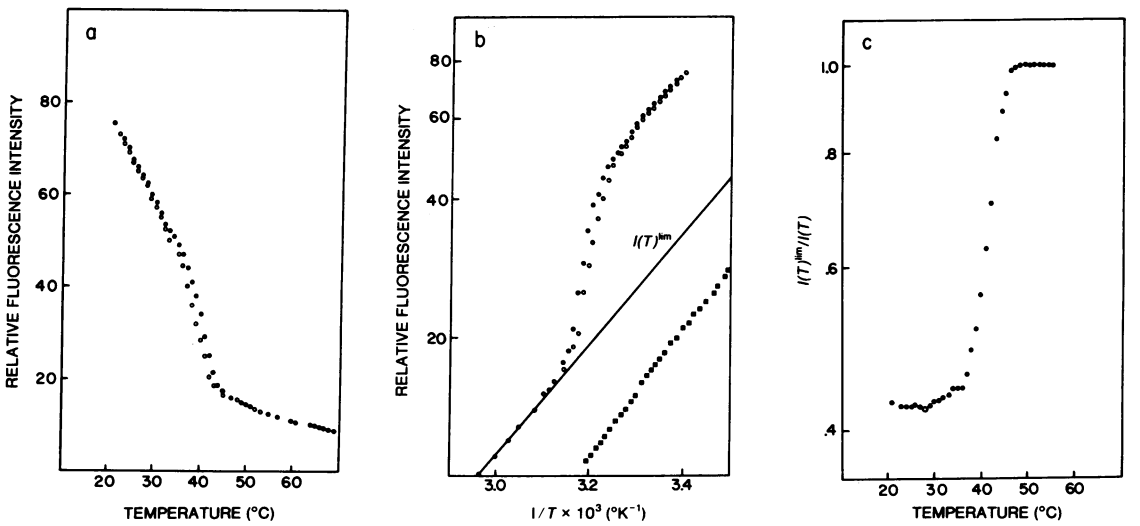

FIG. 3. Determination of Pal_2Lec phase transition by fluorescence of 1-palmitoyl-2-α-parinaroyl lecithin (probe III, $n = 14$). The sample was prepared as described in *Materials and Methods*. Excitation at 320 nm, with a slit width of 1.5 nm and emission at 420 nm with a slit width of 24 nm were used. (a) Fluorescence intensity, $I(T)$ versus temperature. (b) log $I(T)$ versus $1/T$. In both cases, open circles represent decreasing, and closed circles, increasing temperature. The squares (■) show the temperature dependence of the fluorescence of α-parinaric acid (3 μM) in decane determined under similar experimental conditions. The decane data are scaled to approximate its relative quantum yield. The line extrapolated through the high temperature end of the phase transition is designated $I(T)^{lim}$ and has a slope defined as θ^f. There is a small hysteresis (1°C) at the midpoint of the transition. (c) A plot of $I(T)^{lim}/I(T)$ versus temperature for the increasing temperature data. The open circle, I^{min}, represents the minimum value of $I(T)^{lim}/I(T)$.

Model lipids

Aqueous dispersions of diacyllecithins exhibit a sharp change in physical properties through a narrow temperature range known as the phase transition region. A number of physical techniques (1–3, 13–18) have been used to characterize these transitions. The fluid state is accompanied by increased motional freedom which has been correlated with a variety of functional parameters in biological membranes (19).

Fig. 3 shows the progression of data treatment in a typical phase transition measured with linear polyene probes. Fig. 3a is a plot of the fluorescence intensity, $I(T)$, versus temperature for a Pal_2Lec dispersion containing less than 1% (mole fraction) 1-palmitoyl-2-α-parinaroyl-*sn*-glycero-3-phosphoryl-choline (III, $n = 14$). Temperature scans in both directions are shown. Fig. 3b is a plot of the same data as log $I(T)$ versus $1/T$. The regions above and below the phase transition are nearly linear functions of temperature in this plot. The high temperature region for the lipid is nearly parallel to the free fatty acid in decane and is extrapolated along the line labeled $I(T)^{lim}$. The slope of the line, designated θ^f, is defined as the range, in units of $°K^{-1}$, over which the fluorescence intensity doubles. A plot of $I(T)^{lim}/I(T)$ versus temperature, as shown in Fig. 3c, removes this slow variation of the probe fluorescence in the fluid phase. The logarithmic presentation of the data emphasizes the small, but measurable, effect of the pretransition at about 29°. The parameter θ is related to polarizability changes caused by thermal expansion, and it is expected that θ for the solid phase (θ^s) will differ from the liquid phase value (θ^f). The upturn of the low temperature region (see also Fig. 4) indicates that the rate of thermal expansion in the vicinity of the probe in the liquid phase is greater than in the solid phase (the magnitude of θ^f is less than θ^s). The point I^{min} (the open circle in Fig. 3c) represents the maximum ratio of probe quantum yield in the solid to fluid phase, and the magnitude of $1/I^{min}$ is a measure of the relative difference of the probe's environment in the two phases ($1/I^{min} = 1$ indicates no observed transition).

Fig. 4 illustrates normalized phase transitions of aqueous dispersions of diacyllecithins. Normalization is accomplished by forming the quotient $\mathcal{I} = \{[(I(T)^{lim}/I(T)) - I^{min}]/(1 - I^{min})\}$. The temperature at which $\mathcal{I} = 0.5$ is taken to represent the transition midpoint temperature, T_m, as indicated by the probe. We believe that the difference in the curves for Pal_2Lec determined with α- and β-parinaric acid indicates the partitioning of the probe between coexisting phases, and in particular that β-parinaric acid may be concentrated in the solid phase regions. The shapes of the transitions for a particular lecithin are qualitatively similar whether determined by free fatty acid or labeled phospholipid probe.

Table 1 summarizes the phase transition parameters for the phospholipid dispersions. θ^f for α-parinaric acid probes is similar to $\theta = 0.23 \times 10^{-3}$ $°K^{-1}$ for decane. Similar values are obtained for other solvents. The small variation in θ^s is not understood. Variations in transition widths (ΔT) and in transition heights ($1/I^{min}$) probably result from chain length differences between lipid and probe. Lecithin/cholesterol dispersions show increasing transition width and a decreasing transition magnitude (i.e., $1/I^{min}$ decreases) as the mole fraction of cholesterol is increased.

Lipid phase transitions can also be monitored by small shifts in the parinaric acid absorption maxima (data not shown). These shifts can be explained in terms of simple theories of solvent shifts for electronic spectra (4) relating to density-dependent solvent polarizability. The fluorescence of linear polyenes is particularly sensitive to environmental perturbations because the fluorescence involves a symmetry-forbidden transition originating from an excited state that is only slightly lower in energy than a strongly allowed transition (4).

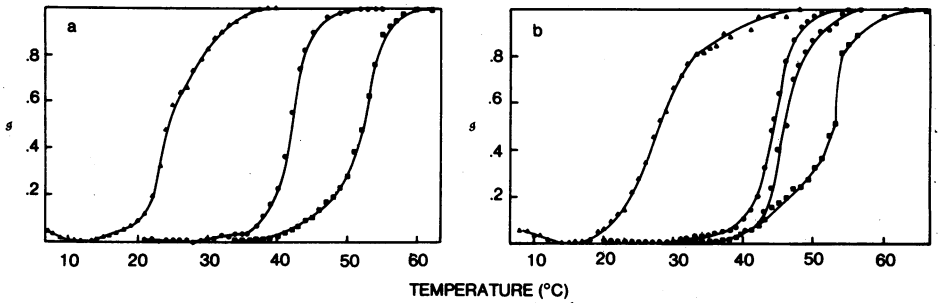

FIG. 4. Normalized phase transition parameter, s, versus temperature for several polyene probes in diacyllecithin dispersions for increasing temperature. (a) s versus temperature for samples containing 0.1% of the appropriate probe of type III in Myr_2Lec (▲), Pal_2Lec (●) (same as Fig. 3), and Ste_2Lec (■). (b) s versus temperature for samples containing 1%, mole ratio, of the free fatty acid probes (I or II) in unlabeled diacyllecithins: α-parinaric acid in Myr_2Lec (▲), Pal_2Lec (●), Ste_2Lec (■), and β-parinaric acid in Pal_2Lec (○).

Lipid–protein interactions

Goodman has characterized the binding of fatty acids to human serum albumin (20). A binding site of high affinity contains an exposed tryptophyl residue (21–23).

Fig. 5a (open circles) illustrates the titration quenching of the fluorescence of the two tryptophyl residues (24) in bovine serum albumin via energy transfer to α-parinaric acid. Quenching occurs because of strong spectral overlap between tryptophan emission and parinaric acid absorption and the proximity of the chromophores on binding. The filled circles in Fig. 5a represent binding of parinaric acid as measured directly by its fluorescence emission. The quantum yield of parinaric acid bound to bovine serum albumin is at least 50 times greater than its value in phosphate buffer.

Fluorescence binding experiments at constant α-parinaric acid concentration (not shown) have been conducted and analyzed in terms of a Scatchard plot. Absorption and difference spectra studies were also carried out. The overall results are similar to that found by Goodman for the interaction of oleic acid with human serum albumin in that there are two strong binding sites ($K \approx 10^6\ M^{-1}$) and three to four weaker binding sites ($K \approx 10^6$–$10^7\ M^{-1}$). There are slight spectral and quantum yield differences for parinaric acid bound to the two classes of sites. Addition of oleic acid displaces α-parinaric acid bound to bovine serum albumin (data not shown).

Fig. 5b shows the circular dichroism spectrum (CD) of parinaric acid bound to bovine serum albumin. Parinaric acid is not optically active, so this spectrum represents CD induced by the asymmetric environment of the protein. This induced CD is very strong and indicates that measurements of this sort should be useful for elucidating lipid–protein interactions.

CONCLUSIONS

The conjugated tetraene fatty acid parinaric acid has been found to be a useful probe for studying lipid–lipid and lipid–protein interactions. Three forms of this probe have been prepared and characterized: two geometrical isomers of the free fatty acid and synthetic phospholipids containing the polyene in the β-position.

Fluorescence and absorption measurements as a function of temperature have shown that these probes can be used to monitor the phase transition of bilayer lipid membranes. The results obtained with the three probe forms are qualitatively similar, but quantitative differences suggest that the α and β forms of the free acid partition differently between the solid and liquid phases.

Lipid–protein interactions can be monitored with parinaric acid by a variety of spectral measurements, including absorption shifts, fluorescence quantum yield increases, tryptophan fluorescence quenching, and induced circular dichroism. This variety of measurements means that different classes of binding sites may be distinguished spectrally as well as on the basis of their binding constants. Studies with bovine serum

TABLE 1. *Summary of phase transition parameters*

Lipid	Probe	$T_{I^{min}}$ (°C)*	T_m (°C)*	ΔT (°C)*	θ'† × 10^3 (°K^{-1})	θ^*† × 10^3 (°K^{-1})	$1/I^{min}$†
Ste_2Lec	α-Parinaric acid	33‡	53	8	0.22	0.25	2.9
	III, n = 16	33‡	52	6	0.25	0.32	2.8
Pal_2Lec	β-Parinaric acid	30	46	4	0.18	0.35	4.8
	α-Parinaric acid	29	44	4	0.22	0.30	3.9
	III, n = 14	29	42	4	0.26	0.30	2.3
Pal_2Lec + 0.1 cholesterol§	III, n = 14	29	40¶	6	0.27	0.30	1.9
Pal_2Lec + 0.3 cholesterol§	III, n = 14	30	42	8	0.25	0.30	1.6
Myr_2Lec	α-Parinaric acid	14	24	9	0.28	0.35	1.9
	III, n = 12	13	22	8	0.24	0.45	1.8

* Uncertainty 1°C. ΔT is the range in °C in which s varies between 0.2 and 0.8.
† Reliable to 10%.
‡ Differs from pretransition results by other methods (13, 17, 18).
§ Mole ratio.
¶ Decreasing temperature scan. Midpoint variation of 1° to 2°.

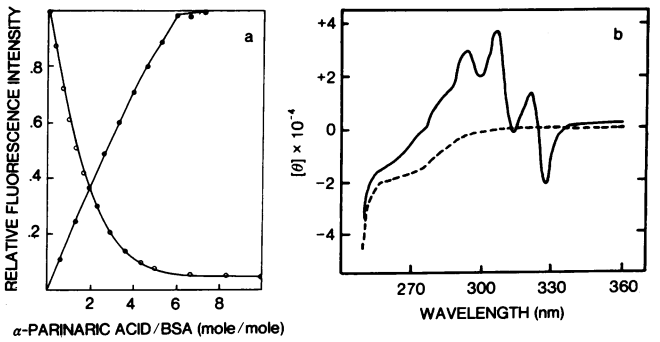

FIG. 5(a). Binding of α-parinaric acid to bovine serum albumin (BSA). Open circles (○) show the quenching of tryptophan fluorescence with increasing amounts of α-parinaric acid. To 25 ml of 0.01 M phosphate buffer, pH 7.4, containing 2.42 mg of albumin (35.0 nmol), were added aliquots of α-parinaric acid in ethanol (2.32 nmol/μl). Excitation of 230 nm (slit width 10 nm) avoids direct excitation of parinaric acid; the emission maximum was near 342 nm (slit width 10 nm). The contribution of tyrosine emission at 342 nm was judged to be small. Direct absorption of tryptophan emission at 342 nm by parinaric acid was minimal. Closed circles (●) show the emission of α-parinaric acid bound to albumin. To 25 ml of 0.01 M phosphate buffer, pH 7.4, containing 1.21 mg of albumin (17.5 nmol), were added aliquots of α-parinaric acid in ethanol (2.32 nmol/μl). The excitation wavelength at 328 nm (slit width 3 nm) and emission maximum near 410 nm (slit width 10 nm) avoids substantial fluorescence from tryptophan. Results have been corrected for the absorption of exciting light by increasing amounts of parinaric acid. In both cases, the solutions were allowed to equilibrate 10 min at 26°C after aliquot addition; the experiments were carried out below the total solubility limits of α-parinaric acid and the presence of small amounts of ethanol (about 0.4% by volume) was determined to have minimal perturbing effects. The fluorescence of free parinaric acid in buffer is less than 2% of bound parinaric acid.

(b) The induced circular dichroism of α-parinaric acid bound to bovine serum albumin. A solution 2.9 μM in BSA and 11 μM in α-parinaric acid (polyene peak absorbance at 310 nm was 0.5) was prepared in pH 7.4 0.01 M phosphate buffer. The solid curve (——) shows the CD of the parinaric acid/bovine serum albumin complex, while the broken curve (- - -) shows the CD of albumin at the same concentration. The complex form of the induced CD curve results from the presence of two low energy electronic transitions in the polyene. Bovine serum albumin, lyophilized and crystallized, and essentially fatty acid-free, was obtained from Sigma Chemical Co.

albumin give results that are similar to those previously published using other techniques.

Recent experimental and theoretical investigations (4) indicate that polyenes may be sensitive to static electric fields as well as other environmental perturbations.

Biosynthetic incorporation of parinaric acid into rats and a fatty acid auxotroph of *Escherichia coli* has been accomplished (manuscript in preparation). These results substantiate the expectation that these probes exert a minimal perturbation of the biological membrane.

We thank Prof. Carl Djerassi for the use of the Jasco J-40, Mrs. Ruth Records for recording the circular dichroism spectra, and Miss Marianne Petersen for her skillful preparation and characterization of β-parinaric acid. This work was supported by National Institutes of Health Research Grants GM 21149 (to B.S.H.) and GM 18539 (to R.D.S.).

1. Radda, G. K. (1971) in *Current Topics in Bioenergetics*, ed. Sanadi, D. R. (Academic Press, New York and London), pp. 81–126.
2. Waggoner, A. S. & Stryer, L. (1970) *Proc. Nat. Acad. Sci. USA* **67**, 579–589.
3. Träuble, H. & Overath, P. (1973) *Biochim. Biophys. Acta* **307**, 491–512.
4. Hudson, B. & Kohler, B. (1974) *Annu. Rev. Phys. Chem.* **25**, 437–460.
5. Kraemer, J. H. (1951) *Trees of the Western Pacific Region* (West Lafayette, Indiana), p. 108.
6. Riley, J. P. (1950) *J. Chem. Soc.*, 12–18.
7. Kaufmann, J. P. & Sud, R. K. (1959) *Chem. Ber.* **92**, 2797–2805.
8. Gunstone, F. D. & Subbarao, R. (1967) *Chem. Phys. Lipids* **1**, 349–369.
9. Cubero Robles, E. & Van Den Berg, E. (1969) *Biochim. Biophys. Acta* **187**, 520–526.
10. Berlman, I. B. (1971) *Handbook of Fluorescence Spectra of Aromatic Molecules* (Academic Press, New York), p. 302.
11. Wu, C. W. & Stryer, L. (1972) *Proc. Nat. Acad. Sci. USA* **69**, 1104–1108.
12. Zechmeister, L. (1962) *Cis-Trans Isomeric Carotenoids, Vitamins A and Arylpolyenes* (Springer-Verlag, Vienna).
13. Hubbell, W. L. & McConnell, H. M. (1971) *J. Amer. Chem. Soc.* **93**, 314–326.
14. Jost, P., Waggoner, A. S. & Griffith, O. H. (1971) in *Structure and Function of Biological Membranes*, ed. Rothfield, L. I. (Academic Press, New York and London), pp. 83–144.
15. Horwitz, A. F. (1972) in *Membrane Molecular Biology*, eds. Fox, C. F. & Keith, A. D. (Sinauer Assoc., Stamford), pp. 164–191.
16. Luzzati, V. & Tardieu, A. (1974) *Annu. Rev. Phys. Chem.* **25**, 79–94.
17. Ladbrooke, B. D., Williams, R. M. & Chapman, D. (1968) *Biochim. Biophys. Acta* **150**, 333–340.
18. Ladbrooke, B. D. & Chapman, D. (1969) *Chem. Phys. Lipids* **3**, 304–367.
19. Fox, C. F. (1972) in *Membrane Molecular Biology*, eds. Fox, C. F. & Keith, A. D. (Sinauer Assoc., Stamford), pp. 345–385.
20. Goodman, D. S. (1958) *J. Amer. Chem. Soc.* **80**, 3892–3898.
21. Swaney, J. B. & Klotz, I. M. (1970) *Biochemistry* **9**, 2570–2574.
22. Wallach, D. F. H., Verma, S. P., Wiedekamm, E. & Bieri, V. (1974) *Biochim. Biophys. Acta* **356**, 68–81.
23. Burstein, E. A., Vedenkina, N. S. & Ivkova, M. N. (1973) *Photochem. Photobiol.* **18**, 263–279.
24. Longworth, J. W. (1971) in *Excited States of Proteins and Nucleic Acids*, eds. Steiner, R. F. & Weinryb, I. (Plenum Press, New York and London), pp. 432–433.